Minimal number of atoms to constitute a magnet: suppression of magnetic order in spherical MnS nanoparticles

T. Kurz, L. Chen, F. J. Brieler, P. J. Klar, Hans-Albrecht Krug von Nidda, M. Fröba, W. Heimbrodt, Alois Loidl

Angaben zur Veröffentlichung / Publication details:

Kurz, T., L. Chen, F. J. Brieler, P. J. Klar, Hans-Albrecht Krug von Nidda, M. Fröba, W. Heimbrodt, and Alois Loidl. 2008. "Minimal number of atoms to constitute a magnet: suppression of magnetic order in spherical MnS nanoparticles." *Physical Review B* 78 (13): 132408. https://doi.org/10.1103/physrevb.78.132408.

Minimal number of atoms to constitute a magnet: Suppression of magnetic order in spherical MnS nanoparticles

T. Kurz,[1] L. Chen,[2] F. J. Brieler,[3] P. J. Klar,[4] H.-A. Krug von Nidda,[1] M. Fröba,[3] W. Heimbrodt,[2] and A. Loidl[1]
[1]*Experimentalphysik V, Center for Electronic Correlations and Magnetism, University of Augsburg, 86135 Augsburg, Germany*
[2]*Department of Physics and Material Sciences Center, Philipps-University, Renthof 5, 35032 Marburg, Germany*
[3]*Institute of Inorganic and Applied Chemistry, University of Hamburg, Martin-Luther-King-Platz 6, 20146 Hamburg, Germany*
[4]*Institute of Experimental Physics I, Justus-Liebig University, Heinrich-Buff Ring 16, 35392 Giessen, Germany*
(Received 25 August 2008; revised manuscript received 17 September 2008; published 17 October 2008)

We have studied the paramagnetic-to-antiferromagnetic phase transition in spherical β-MnS nanoparticles of well defined diameters in the range of 3–11 nm. The MnS nanoparticles were obtained by intrapore synthesis inside mesoporous silica matrices. Electron spin resonance and magnetization measurements reveal that no antiferromagnetic order is established in MnS spheres of 3 nm down to 2 K and that the antiferromagnetic order is gradually recovered on increasing the particle diameter to 11 nm. Photoluminescence excitation spectroscopy proves that in all MnS nanostructures the nearest-neighbor coupling between the Mn ions remains the same as in bulk suggesting that the suppression of the phase transition arises due to geometric restrictions alone.

DOI: 10.1103/PhysRevB.78.132408 PACS number(s): 75.50.Pp, 64.70.Nd, 75.30.Kz, 76.30.−v

Democritus' question,[1] how much the extension of a material can be reduced before losing its natural properties, has been debated for more than 2400 years. For chemical properties, this limit is given by the radii of atoms and molecules. Regarding electronic correlations and magnetism, the question is still up to date, because miniaturization in today's electronics approaches dimensions where quantum effects become more and more important. Ideal one- and two-dimensional systems of Heisenberg type, i.e., characterized by isotropic interaction between the spins, do not develop any kind of long-range magnetic order down to lowest temperatures (Mermin-Wagner theorem[2]). However, the assumptions of this theorem are hard to realize experimentally. Most systems exhibit some residual anisotropy of the interaction between the spins and, furthermore, real magnetic nanostructures usually have finite extensions in all three dimensions, e.g., quantum wires of a finite thickness and length or spherical quantum dots of a finite diameter. Here we address a related problem of high interest both for basic research and application in electronics design and determine the limit, where long-range magnetic order is suppressed, when scaling down a three-dimensional object: We investigate the paramagnetic (PM) to antiferromagnetic (AFM) phase transition of β-MnS nanoparticles incorporated within mesoporous silica hosts.

To study nanoscale effects, it is necessary to precisely control the size of the nanoparticles. Recently, a strong decrease in T_N was found in CuO nanoparticles of diameters $d \leq 10$ nm (Refs. 3 and 4) on the lower boundary accessible by sol-gel preparation or ball milling used in those works. Smaller particle sizes can be obtained using the family of host materials, called M41S phases,[5] which provides ordered arrays of nanotubes with well defined diameters between 3 and 12 nm. These hosts are ideally suited for the incorporation of magnetic semiconductor guest materials (cf. Fig. 1). Consisting of the large band-gap insulator SiO_2, they serve as a barrier material for the semiconductor. In this way, regular arrays of nonmagnetic semiconductor nanostructures[6–11] have been successfully synthesized. In general, the focus in studies of such semiconductor nanostructures is the effect of reduced dimensions on their optical properties[12,13] in comparison to bulk material.

Magnetism can be induced by substituting cations with magnetic transition-metal ions. In this way, the diluted magnetic semiconductors $Cd_{1-x}Mn_xS$ (Ref. 14) and $Zn_{1-x}Mn_xS$ (Ref. 15) have recently been synthesized and analyzed. Here, both optical (band-gap bowing and quantum confinement) and magnetic properties (Curie-Weiss temperature and electron-spin resonance linewidth) were strongly altered upon size reduction. Thereby, the increased surface-to-volume ratio turned out to be decisive in small spherical nanostructures. The influence of the dimension on long-range magnetic order can be studied best using the pure MnS system. MnS exists in three modifications of rock salt, zincblende, and wurtzite type. Here, we concentrate on

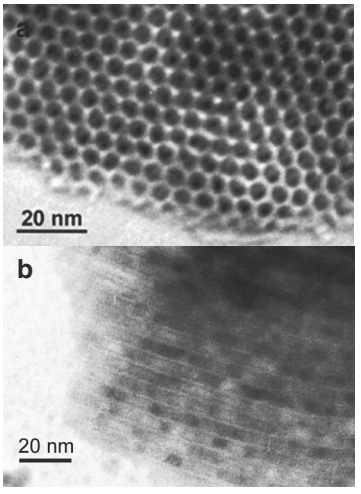

FIG. 1. Transmission electron microscopy (TEM) images: (a) Top view of an empty SiO_2 nanostructure; (b) cut along the channels after filling with the magnetic semiconductor.

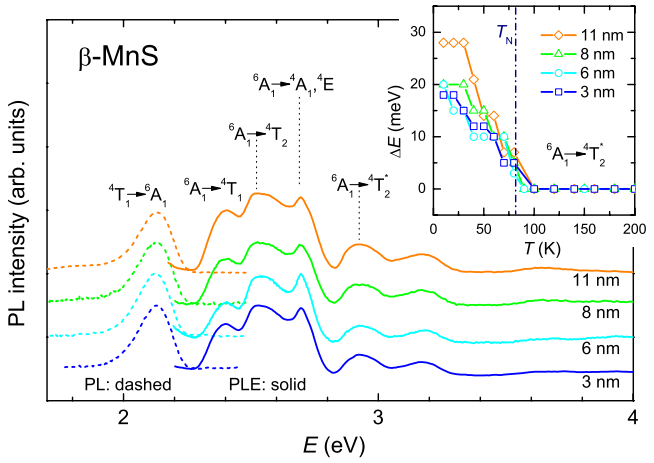

FIG. 2. (Color online) Comparison of PL and PLE results at $T=10$ K in β-MnS nanoparticles of different diameters. Inset: temperature dependence of the energy shift ΔE with respect to room temperature for the ${}^6A_1 \rightarrow {}^4T_2^*$ transition.

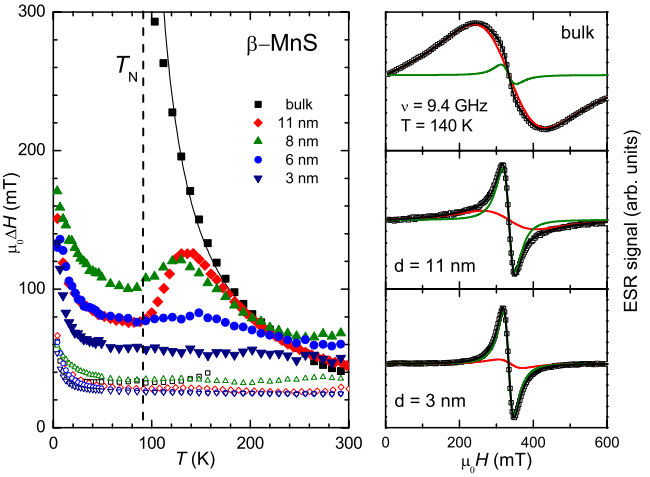

FIG. 3. (Color online) ESR results of β-MnS nanoparticles and bulk. Left: linewidth as a function of temperature; solid symbols: broad line, open symbols: narrow line. Right: ESR signal fitted by two Lorentz lines for bulk and nanoparticles of $d=11$ and 3 nm.

wurtzite β-MnS, which can be characterized as a hcp type III antiferromagnet with a Néel temperature of approximately $T_N \approx 80$ K and a Curie-Weiss temperature of $\Theta=-932$ K.[16] It is highly isotropic in all three dimensions and the spin system can be well described in terms of the Heisenberg Hamiltonian $\mathcal{H}=\Sigma J_{ij}\mathbf{S_i}\mathbf{S_j}$, characterized by isotropic exchange constants J_{ij} between spins $\mathbf{S_i}$ and $\mathbf{S_j}$.[17] Spherical β-MnS particles can be synthesized inside the pores of mesoporous silica hosts at moderate temperatures avoiding reactions with the SiO_2 walls and admixtures of other MnS modifications [cf. Fig. 1(b)]. Details of the synthesis and sample characterization are described in Ref. 15.

The electronic properties of the incorporated MnS nanoparticles were investigated by means of optical and magnetic techniques: photoluminescence (PL) measurements were carried out at 10 K. For PL, excitation light was provided either by a HeCd laser (325 nm) or by a tunable tungsten lamp system followed by a monochromator (470 nm; bandwidth 5 nm). The PL signal was detected in the range from 500 to 700 nm. For photoluminescence excitation (PLE), the PL intensity was detected at 600 nm, varying the wavelength of the excitation light from 270 to 580 nm. The sample luminescence was detected by a spectrometer equipped with a GaAs photomultiplier (resolution better than 1 nm). Optical absorption spectra were recorded in the temperature range $10 \leq T \leq 200$ K using the same setup. Electron spin-resonance (ESR) studies were performed at X-band frequency ($f=9.35$ GHz) and static magnetic fields up to 1 T for temperatures $4.2 \leq T \leq 300$ K. Magnetization measurements have been performed in a superconducting quantum interference device (SQUID) at temperatures $2 < T < 300$ K.

Our optical spectroscopic studies unambiguously prove that the nanostructures are β-MnS. Figure 2 depicts the PL spectra of the MnS nanostructures of various diameters. The so-called yellow emission band centered at about 2.1 eV can be clearly detected. It corresponds to the Mn-internal transition between the first excited ${}^4T_1$ and the ${}^6A_1$ ground state of the Mn $3d^5$ shell in the tetrahedral local environment of β-MnS. The corresponding PLE spectra are typical for this MnS phase and consist of the transitions from the ${}^6A_1(6S)$ ground state to the excited states ${}^4T_1(4G)$, ${}^4T_2(4G)$, ${}^4A_1(4G)$, ${}^4E(4G)$, and ${}^4T_2(4D)$ (abbreviated as ${}^4T_2^*$).[18–20]

Another characteristic property of β-MnS is evident from the temperature dependence of the internal transitions. The inset of Fig. 2 summarizes the energy shifts of the ${}^6A_1 \rightarrow {}^4T_2^*$ transition deduced from absorption spectra of β-MnS nanoparticles of different diameters. The temperature, where the energy shift sets in, is close to the Néel temperature of the bulk material. The magnitude of the shift ΔE for $d=11$ nm is very similar to the bulk value $\Delta E \approx 30$ meV.[20] This is in agreement with earlier observations on bulk wide-gap AFM manganese chalcogenides, where a strong correlation exists between the energy positions of the Mn-internal transitions and the magnetic phase transition from the PM phase into the AFM phase.[20–22] This shift is explained by an exchange effect: the energies of the $3d$ states are lowered because of the alignment of the nearest-neighbor spins. The lowering is larger for the ${}^6A_1$ ground state ($S=5/2$) than for the excited states ($S=3/2$) resulting in an increase in the transition energies.[20] The reduced shift for the smaller particles (see inset of Fig. 2) is caused by the enhanced influence of surface Mn ions with reduced number of nearest neighbors (nn). The observation of this shift in the nanosystems indicates that at least the local AFM correlations, i.e., the nn exchange constant, remains unchanged with respect to the bulk material. However, as we will see from magnetic measurements in the following, long-range magnetic order is strongly affected by reducing the nanostructure size.

ESR operates locally on the magnetic ion and allows for a precise study of the PM$\leftrightarrow$AFM phase transition. For selected samples (bulk, $d=3$ and 11 nm), typical ESR signals are depicted on the right of Fig. 3. All spectra are satisfactorily described by the sum of two Lorentzian lines, a broad and a narrow one. The temperature dependence of the linewidth data is depicted on the left of Fig. 3. The narrow line does not show a significant linewidth dependence (about 30 mT and slightly increasing below 30 K) on pore diameter. In

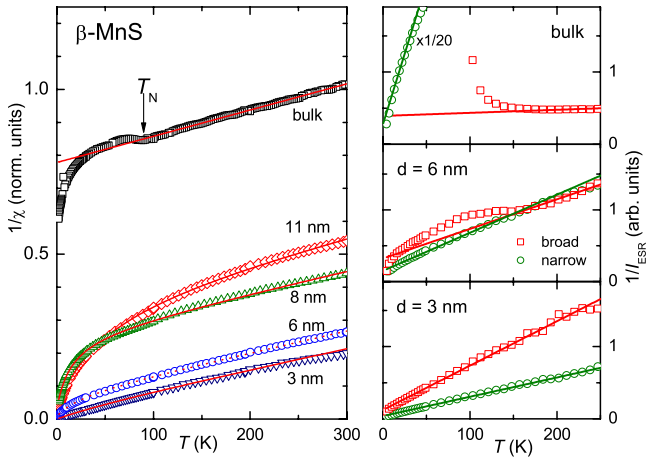

FIG. 4. (Color online) Left: temperature dependence of the inverse SQUID susceptibility for all pore diameters normalized to the same PM moment, because absolute values depend on the degree of filling. Right: inverse ESR intensities of the broad and narrow line for bulk and nanospheres with diameters of $d=6$ and 3 nm.

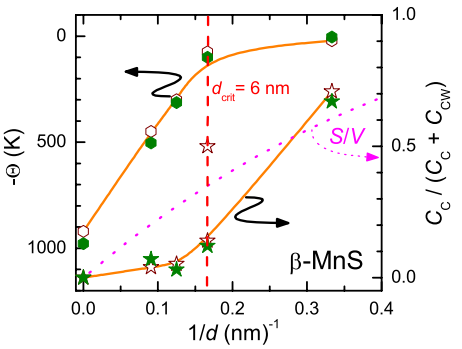

FIG. 5. (Color online) Left axis: Curie-Weiss temperature (hexagons) of β-MnS as a function of inverse pore diameter. Right axis: relative portion (stars) of Curie law with respect to total susceptibility, gained from SQUID (closed) and ESR (open) data, and surface-to-volume ratio S/V (dotted).

contrast, the broad line strongly varies with temperature and dimension. In the bulk system, the linewidth diverges at T_N due to the corresponding decrease in the spin-spin relaxation time,[23–26] which is correlated with the divergence of the correlation length. Assuming a dominant isotropic Heisenberg exchange and a weak (dipolar) coupling as the source of anisotropy, the temperature dependence of the critical part of the linewidth is $\Delta H \propto 1/(T-T_N)^{\gamma}$ (solid line). The critical exponent is found to be $\gamma=1.1$, which is in good agreement with theoretical predictions.[27] This divergence is partially visible for $d=11$ nm as well, but becomes more and more smeared out with decreasing pore diameter. Finally, no indication for such a divergence is found for $d=3$ nm, indicating the suppression of magnetic order due to the reduced particle size.

More information is obtained from the ESR intensity, which corresponds to the local spin susceptibility, as well as from SQUID data which are compared in Fig. 4. The intensity of the narrow line can be described by a Curie law $\chi = C_C/T$ for all samples, whereas the broad line follows a Curie-Weiss law $\chi = C_{CW}/(T-\Theta)$ at high temperatures. To lower temperatures, the broad line becomes undetectable on approaching T_N in the bulk material, as typical for antiferromagnets with an excitation gap larger than the applied microwave frequency. For $d=6$ nm, a sizable part of the signal intensity survives the transition, but for $d=3$ nm the broad line follows the Curie-Weiss law down to the lowest temperature, confirming the complete suppression of magnetic order. Figure 5 compares the quantitative results as a function of inverse particle size. The Curie-Weiss temperatures obtained from the fit of the SQUID data by a sum of a Curie and a Curie-Weiss contribution as well as the relative portions of both contributions correspond well to those determined from the ESR intensities.

At first glance, the observed decrease in Θ with decreasing d and the suppression of the magnetic order seem to be in contradiction to the conservation of the exchange parameter derived from the optical experiments above. To lift this paradoxon, we have to discuss the Curie-Weiss temperature Θ in more detail; it is given by the well-known relationship[28,29]

$$-\frac{k_B\Theta}{2S(S+1)} = \sum_{p>0} J_p z_p \approx J_{nn} z_{nn} + J_{nnn} z_{nnn}, \qquad (1)$$

where J_p is the exchange-coupling constant between a central ion and an ion on the pth-neighbor shell and z_p is the number of neighbors in the pth shell. In bulk material, one commonly uses the approximation up to the second shell where $z_{nn(n)}$ and $J_{nn(n)}$ denote number and exchange constants of (next) nearest neighbors. As the optical experiments indicate that the nearest-neighbor exchange is not altered, the number of neighbors has to change. The only region for this to happen is close to the surface of the nanoparticles. Figure 1(b) shows that, though the majority of the nanospheres has a diameter equivalent to the pore diameter, spherical particles of smaller diameters are also present. The effects due to the vicinity of the surface become more pronounced with decreasing particle size due to the $1/d$ dependence of the surface-to-volume ratio and, hence, reduce the largest possible Curie-Weiss temperature. In total, a distribution of particle sizes with the sharp upper limit d can be assumed. This yields a distribution of Curie-Weiss temperatures between a maximum absolute value $|\Theta_{max}(d)|$ for the particles of size d and $\Theta=0$ K for the smallest particles. Our evaluation of the SQUID susceptibilities and ESR intensities approximates this distribution in the easiest way by two Curie-Weiss laws. In the present case of an antiferromagnet, the small particles dominate at low temperatures (Curie law) whereas the largest particles gain weight with increasing T.

As one can see in Fig. 5, the relative portion of the Curie contribution increases with decreasing pore diameter due to the loss of particles with larger diameters, especially below the critical value of $d_{crit}=6$ nm where the Curie-Weiss temperature approaches zero. Note that the Curie contribution strongly varies for different batches of samples with 6 nm pores, i.e., in this regime, the system is very sensitive to slight changes in the pore diameter. This can be explained via the ratio of surface volume S and total volume V which

we also plotted in Fig. 5, assuming spherical particles with a surface thickness of one nearest-neighbor distance (approximately 0.4 nm). In the range $6>d>3$ nm, this ratio changes from a volume-dominated ($S/V<0.5$) to a surface-dominated behavior ($S/V>0.5$). The long-range order phase transition around the Néel temperature can be followed with decreasing pore diameter in both ESR intensity and linewidth. The largest particles inside the pore system dominate the ESR signal only until they reach the AFM state (because particles in the AFM state do not contribute to the ESR signal). As long as volume-dominated particles are present, they give a divergent contribution to both linewidth and inverse intensity at the Néel temperature. However, their number decreases with pore diameter. As a consequence, the corresponding anomalies become less pronounced and do not shift.

In summary, the magnetic measurements indicate a gradual reduction in the Curie-Weiss temperature and suppression of long-range magnetic order with decreasing diameter of the β-MnS spheres. However, optical measurements show that the short-range exchange interactions in β-MnS are not affected by the reduced dimension. This means that long-range order needs a minimum number of neighbors to provide a volume-dominated environment. By controlled tuning of the pore diameter d in the range of a few nanometers, we were able to determine the crossover between surface-dominated and volume-dominated regimes for spherical β-MnS nanospheres as $3<d<6$ nm. This corresponds to a number of 1000–4000 Mn spins which are necessary to form long-range magnetic order.

We thank Dana Vieweg for susceptibility measurements and Günter Koch for the transmission electron micrographs. We are grateful for funding by the DFG within SFB 484 (Augsburg) and the Optodynamics Center of Philipps University.

[1] Aristoteles: On coming to be and passing away.
[2] N. D. Mermin and H. Wagner, Phys. Rev. Lett. **17**, 1133 (1966).
[3] A. Punnoose, H. Magnone, M. S. Seehra, and J. Bonevich, Phys. Rev. B **64**, 174420 (2001).
[4] X. G. Zheng, T. Mori, K. Nishiyama, W. Higemoto, and C. N. Xu, Solid State Commun. **132**, 493 (2004).
[5] C. T. Kresge, M. E. Leonowicz, W. J. Roth, J. C. Vartulli, and J. S. Beck, Nature (London) **359**, 710 (1992).
[6] T. Hirai, H. Okubo, and I. Komasawa, J. Phys. Chem. B **103**, 4228 (1999).
[7] H. Parala, H. Winkler, M. Kolbe, A. Wohlfahrt, R. A. Fischer, R. Schmechel, and H. von Seggem, Adv. Mater. (Weinheim, Ger.) **12**, 1050 (2000).
[8] V. I. Srdanov, I. Alxneit, G. D. Stucky, C. M. Reaves, and S. P. DenBaars, J. Phys. Chem. B **102**, 3341 (1998).
[9] J. R. Agger, M. W. Anderson, M. E. Pemble, O. Terasaki, and Y. Nozue, J. Phys. Chem. B **102**, 3345 (1998).
[10] R. Leon, D. Margolese, G. Stucky, and P. M. Petroff, Phys. Rev. B **52**, R2285 (1995).
[11] Y. S. Tang, S. Cai, G. Jin, J. Duan, K. L. Wang, H. M. Soyes, and B. S. Dunn, Appl. Phys. Lett. **71**, 2448 (1997).
[12] R. N. Bhargava, J. Lumin. **70**, 85 (1996).
[13] A. D. Yoffe, Adv. Phys. **42**, 173 (1993).
[14] F. J. Brieler, P. Grundmann, M. Fröba, L. Chen, P. J. Klar, W. Heimbrodt, H.-A. Krug von Nidda, T. Kurz, and A. Loidl, Chem. Mater. **17**, 795 (2005).
[15] F. J. Brieler, P. Grundmann, M. Fröba, L. Chen, P. J. Klar, W. Heimbrodt, H.-A. Krug von Nidda, T. Kurz, and A. Loidl, J. Am. Chem. Soc. **126**, 797 (2004).
[16] L. Corliss, N. Elliott, and J. Hastings, Phys. Rev. **104**, 924 (1956).
[17] A. Danielian and K. W. H. Stevens, Proc. Phys. Soc. London **77**, 124 (1961).
[18] O. Goede and W. Heimbrodt, Phys. Status Solidi B **146**, 11 (1988).
[19] O. Goede, W. Heimbrodt, and V. Weinhold, Phys. Status Solidi B **136**, K49 (1986).
[20] W. Heimbrodt, C. Benecke, O. Goede, and H.-E. Gumlich, Phys. Status Solidi B **154**, 405 (1989).
[21] W. Heimbrodt, C. Benecke, O. Goede, and H.-E. Gumlich, J. Cryst. Growth **101**, 911 (1990).
[22] M. S. Seehra and R. D. Groves, J. Phys. C **16**, L411 (1983).
[23] K. Kawasaki, Prog. Theor. Phys. **39**, 285 (1968).
[24] H. Mori and K. Kawasaki, Prog. Theor. Phys. **28**, 971 (1962).
[25] D. L. Huber, Phys. Rev. B **6**, 3180 (1972).
[26] S. Maekawa, J. Phys. Soc. Jpn. **33**, 573 (1972).
[27] O. Goede, D. Backs, W. Heimbrodt, and M. Kanis, Phys. Status Solidi B **151**, 311 (1989).
[28] J. K. Furdyna, N. Samarth, R. B. Frankel, and J. Spalek, Phys. Rev. B **37**, 3707 (1988).
[29] C. J. Chen, M. Qu, W. Hu, X. Zhang, F. Lin, H. B. Hu, K. Ma, and W. Giriat, J. Appl. Phys. **69**, 6114 (1991).